Clinical Neurophysiology 130 (2019) 1342–1350

Contents lists available at ScienceDirect

Clinical Neurophysiology

journal homepage: www.elsevier.com/locate/clinph

Probabilistic graphical model identifies clusters of EEG patterns in recordings from neonates

A. Sarishvili [a,1], J. Winter [b,*,1], H.J. Luhmann [c], E. Mildenberger [b]

[a] Fraunhofer Institute for Industrial Mathematics, Kaiserslautern, Germany
[b] Department of Neonatology, University Medical Center of the Johannes Gutenberg University Mainz, Germany
[c] Institute of Physiology, University Medical Center of the Johannes Gutenberg University Mainz, Germany

ARTICLE INFO

Article history:
Accepted 6 April 2019
Available online 11 May 2019

Keywords:
Brain monitoring
Electroencephalography
Automated detection
Neonate
Chow-Liu tree
Multi-dimensional scaling

HIGHLIGHTS

- Analysis of multivariate EEG signals in frequency domain resulting in construction of Chow-Liu trees.
- Visualization of energy interplay in EEG channel frequency band combinations.
- Correlation of graph edit distances of estimated 3d Chow-Liu tree with medical classification of EEG.

ABSTRACT

Objectives: In this paper we introduce a novel method for the evaluation of neonatal brain function via multivariate EEG (electroencephalography) signal processing and embedding into a probabilistic graph, the so called Chow-Liu tree.
Methods: Using 28 EEG recordings of preterm and term neonate infants the complex features of the EEG signals were constructed in the form of a Chow-Liu tree. The trees were embedded into a 3 dimensional Euclidean space. Clustering of specific EEG patterns was done by complete linkage algorithm.
Results: Our analytic tool was able to build clusters of patients with pathological EEG findings. In particular, we were able to make a visual proof on a 3d multidimensional scaling coordinate system with a good performance. The distances (graph edit distance) between Chow-Liu trees of different infants were proportional to the clinical findings of corresponding infants.
Conclusion: Our method may provide a basis for the future development of a diagnostic/prognostic non-invasive brain monitoring tool which will be able to differentiate between a variety of complex clinical findings.
Significance: This model addresses relevant issues in neonatology and neuropediatrics in terms of identification of possible clinical factors which interfere with normal brain development and will allow fast unbiased recognition of infants with specific pathological EEG findings.

1. Introduction

Brain function monitoring in neonates during their stay in the neonatal intensive care unit (NICU) may be a valuable tool to evaluate brain development in infants and to investigate factors interfering with brain development (Gressens et al., 2002, Perlman, 2001). Evaluating changes in EEG patterns is useful in the prediction of long-term outcome of neonates (Watanabe et al., 1999) and acute and chronic EEG changes correlate with later neurological and cognitive function (Hellstrom-Westas and Rosen, 2005).

Typical neonatal EEG patterns and signals of electrical activity change as a function of gestational age (GA) and postmenstrual age (PMA, GA + postnatal age) (Andre et al., 2010). EEG patterns which occur delayed in relationship to the actual PMA are called dysmature (Lombroso, 1985). Dysmature EEG patterns have been related to adverse outcome later in life (Hayakawa et al., 1999, Pezzani et al., 1986). Hayakawa et al. identified "disorganized" patterns, following an acute brain insult, and related them to white matter injury, motor outcome and "dysmature" patterns, demonstrating deviations in neurodevelopment associated with grey

* Corresponding author at: University Medical Center of the Johannes Gutenberg University Mainz, Langenbeckstr. 1, 55131 Mainz, Germany. Fax: +49 6131173477.
E-mail address: julia.winter@unimedizin-mainz.de (J. Winter).
[1] Both authors contributed equally to this paper.

https://doi.org/10.1016/j.clinph.2019.04.708
1388-2457/

matter injury and cognitive outcome (Okumura et al., 2002, Watanabe et al., 1999).

To simplify the information complexity presented in the EEG signal and in order to visualize clinically relevant features that can be interpreted by less experienced clinical staff and to monitor EEG changes more objectively and uniformly, automated quantitative neonatal EEG analysis may be valuable. Computer analysis of EEG will allow an objective and reproducible analysis for long-term prognosis and/or stratification of clinical treatment.

In this paper we present a novel method for objective and quantitative EEG analysis which constructs a complex probabilistic graph (Chow-Liu tree) (inter-channel-frequency-band dependency structure) from a given multi-channel EEG recording, for the purpose of the development of an analytic tool to estimate the different generic neonatal brain states. By applying the Chow-Liu method to the analysis of EEG recordings, all characteristics of the EEG signal and their interdependencies can be constructed in a graphical model. We tested the analytic algorithm by using EEG recordings of 28 neonates and aimed to visualize the dependency structure of the EEG signals in the frequency domain in order to assign complex feature graphs of the preterm and term infants. Using this approach, we were able to identify clusters of physiological and pathophysiological EEG patterns.

The aims of our study were:

- To search for significant dependencies between spectral powers in different frequency bands in different channels (12 channels from standard 10–20 electrode positioning system).
- To embed this dependency structure into a probabilistic graph.
- To prove that clustering which is based on distances (degree of dissimilarity) between graphs of different infants correlate with clinical findings.

2. Methods

2.1. Mathematical model

Fig. 1 shows the applied mathematical algorithm. From the 12 channels EEG-recording the method estimates a spectrogram via short time Fourier transformation (steps 1 to 3) (see Appendix A1 for details). In the fourth step the spectrogram is dissected in different frequency bands and the power in each band for each channel is discretized on an ordinal scale in four groups (step 5). In step 6 and step 7 the Chow-Liu tree is estimated (for details see Appendix A2). In step 8 the estimated Chow-Liu trees are pruned by redundant vertices using estimated Chow-Liu trees log-likelihoods (for detail see Appendix A2). In step 9 the graph (Chow-Liu tree in our case) can be transformed into another one by a finite sequence of graph edit operations. Graph edit distance (GED) is defined by the least-cost edit operation sequence. In previous studies (e.g.(Gao et al. (2010))) the edit operations are differentiated between edge insertion and deletion, node insertion and deletion and node substitution. Because the Chow-Liu tree in our application have a fixed structure, i.e. 12 channels and 12 frequency band layers (144 nodes), we only consider edge deletion and edge insertion graph edit operations. We calculated for each pair of patients (there are 378 unique pairings of 28 different patients) the minimal number of graph edit operations needed to

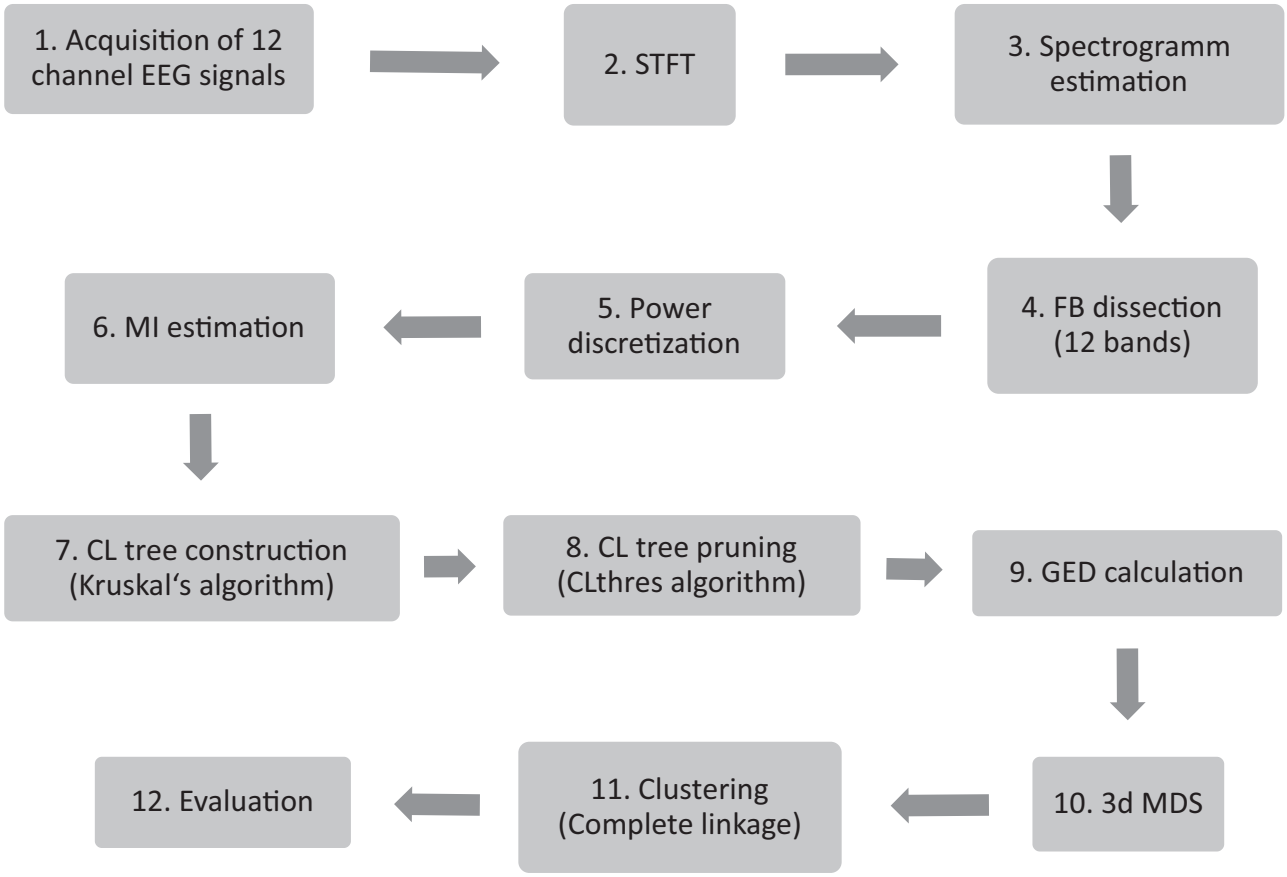

Fig. 1. Flow diagram of the mathematical method. STFT (Short time Fourier transform), MI (Mutural information), FB (Frequency band), CL tree (Chow Liu Tree), GED (Graph edit distance), MDS (Multi dimensional scaling).

transform one dependency graph (Chow-Liu tree) into another. After that, we weighted this number with the mutual information of edges which have been involved into the graph edit operations and subsequently calculated the GED between them. In this manner we obtained the adjacency matrix of all patients in the data base. To visualize the GED between the patients and to establish a link between clusterings derived from the mathematical model and from patient condition we made multidimensional scaling (step 10). The goal of multidimensional scaling analysis is to find a spatial configuration of objects when the known information is the general proximities between them. The proximities indicate the overall dissimilarities of the objects under investigation. Multidimensional scaling spatially configures the objects in a lower dimensional space so that the distances between these objects match their proximities as close as possible.

The points in this 3d coordinate system were clustered in step 11. We clustered the data with the complete linkage algorithm and choose the number of clusters by silhouette principle. The silhouette value is a measure of how similar an object is to its own cluster compared to other clusters. The average value of all silhouette values is then used to quantify the performance of many different clusterings. In our case we compared clustering coming from the same algorithm but with different number of clusters. For the purpose of better illustration of identified cluster shapes, we estimated empirical probability distribution function of the points and cluster centroids in the 3d multidimensional scaling (MDS) space by the multivariate kernel density estimator with Gaussian kernel, sampled the data from this distribution and plotted only the points with high sampling probability. We calculated number of clusters in the range of 3 to 12. By this algorithm 6 clusters have been identified as optimal.

In step 12 the method has been evaluated by comparing the clustering result with the clustering result from the clinical point of view.

2.2. Data collection

EEGs were recorded with sampling rate of 256 Hz and included 12 channels with positioning according to the international 10–20 standard. The 12 channels for analysis were: FP1, FP2, F3, F4, P3, P4, O1, O2, F7, F8, T5, and T6. The EEG recordings were performed with devices from Schwarzer / Natus Europe (formerly it med, Pleasanton, CA 94566 USA). The standard filters were: high-pass filter / time constant 0.3 s, low-pass filter 70 Hz. The duration of recording was between 30 and 70 minutes, depending on the sleep behavior of the children. Brain states of children are included in Table 1. Clinical artifact recognition had been performed by the pediatric neurologist, such that cleaned signals were analyzed.

In total, multichannel EEG recordings from 28 infants were enrolled. Only EEG recordings derived between a PMA of 37 + 0 until 44 + 0 gestational weeks (term age) were included in analysis. The included EEGs had been recorded in the department of neonatology and in the department of pediatric neurology at the University Medical Center Mainz as medically indicated. The use of these anonymized retrospective EEG recordings was approved by the ethics committee of Rhineland-Palatinate, Germany.

In a first step EEG recordings of 18 infants (9 female and 9 male) were analyzed. All 18 EEG recordings had been interpreted by a pediatric neurologist as normal. All the children had no chronic disease. Mean GA was 40.3 weeks with standard deviation of 1.73. PMA at the time of EEG recording varied between 38 + 0 and 43 + 3 weeks.

In a second step EEG recordings of 5 infants with chronic disease were analyzed by the algorithm. Mean GA of the 5 male newborns was 37.1 and PMA at the time of EEG recording varied between 37 + 4 and 43 + 3 weeks. All EEG recordings had been interpreted as normal by a pediatric neurologist.

In a third step the EEG recordings of 5 infants with chronic underlying diseases and pathological EEG findings were analyzed. Mean GA was 41.1 weeks (2 female and 3 male newborns). PMA of the infants at the time of EEG recording varied between 39 + 0 and 42 + 1 weeks.

In total, 28 infants (mean GA 39.0 weeks; 7 preterm infants and 21 full-term infants, 11 female and 17 male) were included in the analysis (for details see Table 1).

3. Results

Analysis of different length of EEG recordings (6, 10, 12, 17.5 and 20 minutes of EEGs) for each of the 28 patients showed stable structure (constant tree topology by increasing the number of data used for parameter estimation) of Chow-Liu trees for EEG recordings longer than 12 minutes for each of the 28 patients (i.e. extension of the analyzed signal length longer than 12 minutes did not increase information content) (see Appendix A3 for details).

The Chow-Liu trees in Fig. 2a and Fig. 2b are representative examples from two patients selected from the data base of 28 infants. The Chow-Liu trees show 144 nodes (random variables indicating energies in corresponding EEG channel frequency band combinations), resulting from 12 EEG channels times 12 frequency bands. Furthermore, the red vertices are indicating the dependencies between corresponding nodes of the graphs. At first sight we observe the basic difference in the orientation of the main (thick) vertices. The patient corresponding to Fig. 2a (ID 16) has an EEG interpreted as normal and his Chow-Liu tree is characterized with horizontal vertices in low frequency bands and few vertical vertices in high frequency bands. Also, the tree weight (sum of estimated mutual information of all vertices of the tree) in Fig. 2a is high in comparison to the Chow-Liu tree weight in Fig. 2b. The Chow-Liu tree of the patient corresponding to Fig. 2b has an EEG recording interpreted as pathologic (ID1) and his Chow-Liu tree is characterized with vertical vertices and low Chow-Liu tree mass (FW of 44.64 in comparison to 95.74 Chow-Liu tree Fig. 2a).

After the application of the described analytical tool on all 28 patient EEG data sets, we obtained a Chow-Liu tree for each patient. We computed the distances between trees (sum of tree edits operations, i.e. removing edge and adding edge operations till translation of one tree into another tree. The tree edit operations have been weighted by the corresponding estimated mutual information). After embedding them into the 3d Euclidean space, we have found that we got a more than acceptable stress parameter of 0.12. The stress parameter is estimated as the square root over the sum of the squared deviations between distances and disparities divided by the sum over squared distances, and therefore is a normed measure of the accuracy or goodness of fit, respectively, of the model; see Kruskal's thumb rules (Kruskal, 1958). We visualized the recordings of individual infants on this coordinate system (see Fig. 3), which also depicts the clustering result. We obtained 6 clusters, which have been identified as optimal for the 28 patients.

Cluster 1 (red) is based on 4 pathological EEG recordings of infants with neurological abnormalities. One infant with a large intraventricular hemorrhage (IVH IV°) and hypsarrhythmia (ID1), one with neonatal seizures (ID7) one preterm infant with a congenital CMV infection (ID9) and one infant with a hypoxic ischemic encephalopathy (ID14). The fifth patient with a hypoxic ischemic encephalopathy and a pathological EEG was merged to cluster 3 (see below).

In cluster 2 (black) all 3 neonates had normal EEG recordings, but 2 of them had underlying chronic diseases (double outlet right ventricle (ID2) and postasphyctic diseases with periventricular

Table 1
Patient characteristics with patient number (ID), gestational age (GA), sex, post menstrual age (PMA), diagnosis and clinical classification of the EEG recordings sorted by clusters identified by the system.

ID	GA	Sex	PMA	Diagnosis	Indication for EEG	EEG result	Brain state
	Cluster 1 (red)						
1	36+6	m	39+0	Prematurity, IVH IV°, PVL, Hydrocephalus e vacuo	IVH IV°	pathologic	non-REM and REM-sleep
7	39+0	f	40+5	Neonatal epileptic seizures	Clinical seizure	pathologic	sleep (Phenobarbital)
9	32+5	f	42+1	Prematurity, cytomegalovirus infection, atrial flutter	Clinical seizure	pathologic	non-REM and REM-sleep
14	37+5	m	39+4	Asphyxia	Hypoxic ischemic encephalopahy	pathologic	sleep (Phenobarbital)
	Cluster 2 (black)						
2	40+1	m	40+1	Double outlet right ventricle, diaphragmatic Hernia		normal	REM-sleep
11	32+5	f	38+2	Prematurity, ABHS	IVH I°, suspected seizure	normal	non-REM and REM-sleep
26	32+6	m	39+4	Prematurity, asphyxia, respiratory distress syndrome	HIE	normal	wake and sleep
	Cluster 3 (yellow)						
3	38+6	m	41+5		ALTE	normal	non-REM and REM-sleep
4	36+4	m	41+3	Prematurity, SGA, early onset sepsis, suspected PVL	ALTE	normal	non-REM and REM-sleep
5	41+0	f	42+5		ALTE	normal	non-REM and REM-sleep
6	38+6	f	40+4	SGA, perinatal acidosis	Drug addicted mother	normal	non-REM and REM-sleep
10	38+6	f	40+5	Early onset Sepsis	Muscular hypotonia	normal	non-REM and REM-sleep
12	39+3	m	41+1	Asphyxia	HIE	pathologic	non-REM and REM-sleep
	Cluster 4 (cyan)						
18	36+0	f	39+2	Prematurity	Hypopnoe, cyanosis	normal	non-REM and REM-sleep
19	37+6	m	38+3		Macrocephalus	normal	non-REM and REM-sleep
20	36+1	m	38+0	Prematurity	Muscular hypotonia	normal	non-REM and REM-sleep
	Cluster 5 (blue)						
16	38+4	m	40+0		Suspected seizures	normal	non-REM and REM-sleep
17	40+4	m	41+2	Postnatal respiratory distress, Pneumothorax	Perinatal acidosis	normal	non-REM and REM-sleep
23	39+3	f	42+6	Acute febrile enterovirus infection	ALTE	normal	non-REM and REM-sleep
22	37+1	m	38+2	SGA, perinatal azidosis	Moderate HIE	normal	sleep
28	38+5	f	39+2	Perinatal acidosis	Apnea	normal	non-REM and REM-sleep
24	37+2	m	38+5	Postnatal respiratory distress	Apnea	normal	wake and sleep
25	36+5	m	37+4	Prematurity, Silver Russel syndrome	Post resuscitation	normal	wake and sleep with sedation
	Cluster 6 (magenta)						
8	35+5	m	42+2	Prematurity, partial trisomy 20, central hypothyreosis	Myoclonia,	normal	non-REM and REM-sleep
13	39+2	m	43+3	Aortic valve stenosis	Post resuscitation	normal	non-REM and REM-sleep
15	37+4	f	39+4		ALTE	normal	non-REM and REM-sleep
21	42+0	m	43+3		ALTE	normal	sleep
27	37+6	f	40+3	Small for gestational age	ALTE	normal	wake and sleep

Periventricular leukomalacia (PVL), Apparent life threatening event (ALTE), Apnoe bradycardia hypoxemia syndrome (ABHS), Intraventricular hemorrhage (IVH), Small for gestational age (SGA), Hypoxic ischemic encephalopathy (HIE).

leukomalacia (ID26)). The third neonate is a preterm infant ((ID11) 32 + 5 weeks of gestational age), who revealed a grade I intraventricular hemorrhage without clinical relevance. The distance between cluster 2 and all other clusters is the furthest.

In cluster 3 (yellow) the system represented 6 EEG samples (5 normal recordings and 1 pathological recording). Besides one infant, all were infants without underlying chronic diseases. The sick infant (ID12) had symptoms of hypoxic ischemic encephalopathy and a pathological EEG recording. The EEG of 3 infants had been recorded because of an apparent life threatening event (ALTE) (IDs 3, 4, 5). One infant showed withdrawal symptoms related to mother's drug consumption during pregnancy (ID6). One infant had a bacterial infection (ID10).

Cluster 4 (cyan) included 3 patients (IDs 18, 19, 20) with normal EEG recordings. 2 were preterm infants (gestational age 36 + 0 and 36 + 1 weeks (ID18 and 20)). The reason for EEG recording had been muscular hypotonia and hypopnea, respectively. One infant had macrocephalus (ID 19).

Cluster 5 (blue) included 7 infants (IDs 16, 17, 22, 23, 24, 25, 28) with normal EEG findings. Reasons for EEG recording in this cluster were ALTE (ID23) or suspected seizures (ID 16) as well as moderate hypoxic ischemic encephalopathy (ID 22). 2 had respiratory dis-

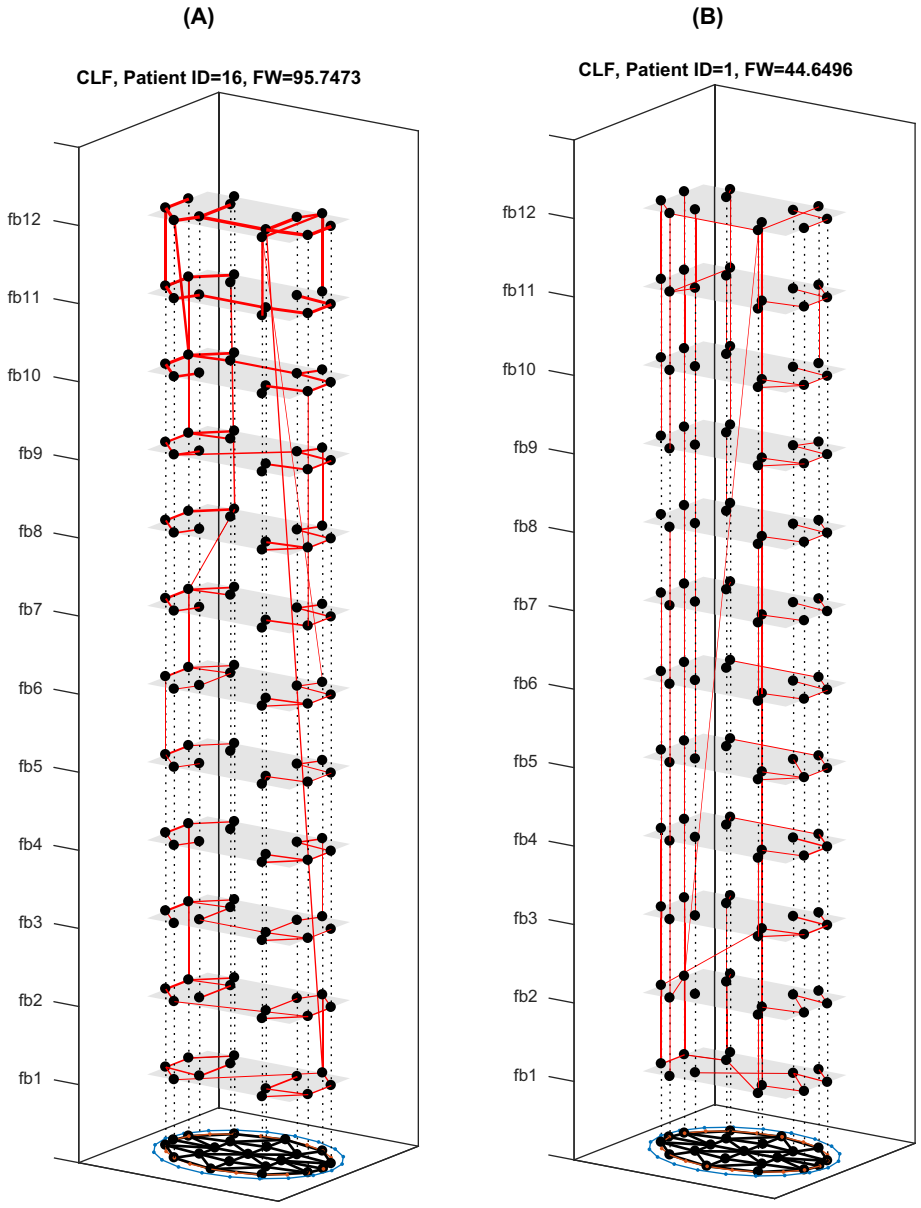

Fig. 2. a/b: Chow-Liu tree generated with 12 channels and 12 frequency bands. The frontal channels are depicted on the left, in the direction of the y axis. The corresponding frequencies can be drawn from Fig. A1. Fig. 2a is a Chow-Liu tree from a patient with a normal EEG (ID 16). Fig. 2b is a Chow-Liu tree from a patient with a pathologic clinical EEG classification (ID1). Red lines indicate the Chow-Liu tree edges. The thickness of the lines is proportional to the strengths of corresponding mutual information. The weight of the tree is the sum of all mutual information of active edges (FW). The gray surfaces indicate the different frequency band level of the Chow-Liu tree. In general, we observed that Chow-Liu trees of EEG recordings clinically classified as pathological had more massive edges in vertical direction (cross frequency band energy couplings in frontal channels) and the normal patients had more edges in horizontal direction (cross channel energy couplings).

tress syndrome (ID 17 and 24). One infant had apnea following perinatal acidosis (ID 28). One infant had a Silver Russel syndrome (ID 25).

Cluster 6 (magenta) summarizes 5 infants (IDs 8, 13, 15, 21, 27) with normal EEG findings. Two infants (ID 8 and 13) showed an underlying chronic disease (aortic valve stenosis and partial trisomy 20), two EEGs had been recorded because of an ALTE (ID 15 and 21), one of a small for gestational age neonate (ID 27).

Fig. 4 is the qualitative visualization of the distances between the different cluster centroids of all children. The figure allows getting a better idea how the identified clusters are distributed in the 3d MDS Euclidean space.

Regarding the distances of cluster centers, the clusters comprising the majority of normal EEG findings were close together (cluster 4, 5 and 6, blue, magenta and cyan, see Fig. 3). The group of pathological recordings showed the highest distance to these clusters. The cluster to which the algorithm merged another pathological recording (ID 12, in the third cluster) showed lower distances to the cluster of infants with pathological EEG recordings, as well as the cluster of infants with underlying diseases and of the preterm infant (cluster 2).

4. Discussion

Automated classification of EEG recordings is a very complex issue, especially if EEG recordings of neonates are to be analyzed. In the clinical practice, neurologists use atlases and the experience that they have acquired from visual evaluation. Developing an assessment system for neonatal EEG means a more objective method to evaluate EEG recordings. In this first study we con-

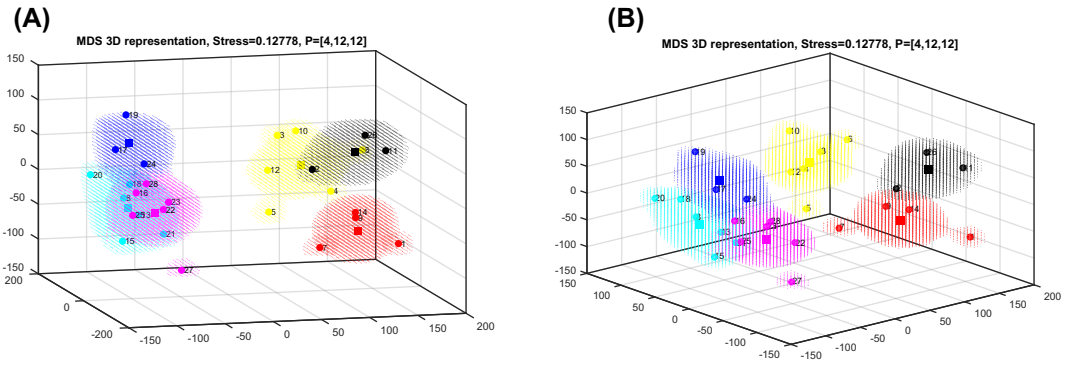

Fig. 3. a/b: The dependency structure between energies of 12 EEG signals in 12 different frequency bands are estimated via Chow-Liu trees for each patient. The distances between trees are then embedded into the 3d Euclidean space using multidimensional scaling (MDS) technique. The points are then clustered by complete linkage. The squares are the centroids of the identified clusters. The distances of the clusters and cluster separation performance of the approach are visualized by two different view angles on the same figure.

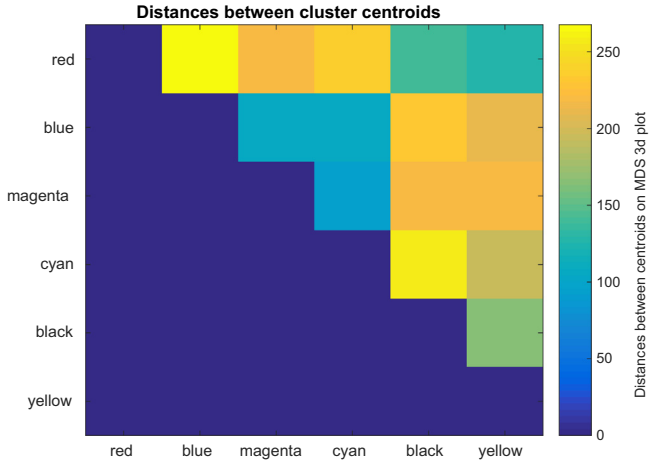

Fig. 4. Distances between cluster centroids. This figure shows the extent to which the different clusters are separated from one another. From nearby clusters (blue shades) to clusters located far from one another (yellow shades). See color scale at the edge.

structed a simple method to identify significant dependencies between spectral powers in different frequency bands in different channels of 12 channel EEG recordings of newborn infants. We were able to embed this dependency structure into a probabilistic graph and to show that clusterings which are based on distances (degree of dissimilarity) between graphs of different infants may correlate with clinical findings. Our tool, unlike previous analysis tools, is multidimensional, combining both quantitative and qualitative aspects. It examines general criteria seen in differences between individual Chow-Liu trees. The advantage of the system is that it works as a self-learning system based on a library. Each analyzed record makes the system more reliable. Here we distinguish between two main system reliability levels:

1) Reliability in the estimated Chow-Liu-trees (see Appendix A3). On this level, system reliability depends on the EEG data quality and EEG recording length for each patient.
2) Reliability in MDS space clustering. On this level, the system reliability depends on the system reliability on first level and on the number of patients in the data base.

Establishing relationship in complex feature space (which has been identified by multi-channel EEG analysis in frequency domain) between infants and identifying correlations between distances and pathological findings of infants may be a real added value of the presented system in comparison to other similar approaches known so far to us. Most existing studies on EEG maturation made use of qualitative visual inspection. Meanwhile some digital EEG recorders provide the opportunity to analyze the EEG signals quantitatively. Some assessed the amount of electrical activity to show for example frequency-dependent differences in performance with sleep state (Curzi-Dascalova et al., 1993) and differences between term and preterm infants (Scher et al., 1994). Victor et al. (Victor et al., 2005) used automated spectral analyses of EEG frequencies to quantitatively describe the EEG of preterm infants just after birth. West et al. (West et al., 2006) analyzed changes in continuity, amplitude, and spectral edge frequency by using automated spectral analysis. In the work of Tort et al. (Tort et al., 2010) scientists quantified the degree of phase-amplitude couplings between high frequency oscillation amplitudes with the phase shift of low frequencies. The modulation of gamma amplitude by the theta phase in the hippocampus was shown in (Canolty et al., 2006). The correlation of phase-amplitude coupling with the inter laminar synchrony were shown in (Ryan et al., 2012). Mormann et al. (Mormann et al., 2000) have shown the correlation between the degree of phase synchronization measured by phase coherence and the pathological activity in epilepsy patients.

Our novel analysis tool contrasts to all methodological approaches described above, as it considers differences / similarities between individual EEG recordings in order to cluster them in a mathematically derived optimal manner. It constructs multivariate graphical features based on the dynamic interaction of the energy content of certain frequency bands / different EEG-channel combinations, in order to derive the individual signature of the brain activity. In addition, the visualization of the patient EEG database in an euclidean 3D space for the detection of patient clusters with similar signatures of graphical features is a unique feature. In addition, by accessing EEG data from other databases (e.g. hospital information system or freely accessible cloud-based EEG data), the system could adapt the existing similarity structures and increase the significance of clustering through identifiable patterns in the sense of a "self-learning" system. The used mathematical approach makes our analysis tool very robust against artifacts. First, it works on band passed signals and it eliminates any outliers in terms of high-power peaks by discretizing windowed EEG data in frequency domain (see method section first paragraph). Second, the Chow-Liu algorithm is very robust on itself. Before building of tree structures it sorts the estimated empirical mutual information of all edge pairs and selects the most significant pairings. The redundant connections are removed from further considerations immediately.

In a first approach, by the analyses of 28 existing retrospective EEG recordings, the new system appears to be able to identify clusters of patients in the 3d space. The method seems to be precise in identifying pathological EEG findings and is able to distinguish pathologic EEG findings diagnosed by a pediatric neurologist from the majority of the normal findings (see cluster 1 in Fig. 3). The method identified also other clusters of EEG recordings that apparently have similar structures. For example, we found similarity in a group of premature infants and infants with chronic diseases in cluster 2. Although our system shows first proof of concept, it is difficult to make clear assignments to specific patient characteristics except for the group of those with pathological EEG findings, because the use of retrospective data limits the precise evaluation. Currently, recognition of similarities and dissimilarities between individual EEG recordings are possible. This opens the possibility of clustering EEG records apart from categories applied so far. The system actually does not serve to issue specific diagnoses or symptoms; however, this is subject of a planned validation study.

We have also to take into account, that the study is limited also by other methodological issues. The number of patients, in particular the number of preterm infants, is small. The EEG samples had not been recorded according to a standardized protocol (different electrodes, nurses, reposition of electrodes). Due to a lack of structural follow up of patient's outcome findings and due to the small sample size it was not possible to identify more and precise detailed medical diagnosis specific clusters on the 3d MDS space.

However, our system has the potential to get easily accessible bedside information about brain maturation and to identify possible clinical factors or special clinical interventions that interfere with normal brain development.

The approach allows modifications/improvements in different directions and can be considered as the basis for many different systems. In particular, the following modifications seem to be promising to us:

1) The approach can be modified/improved regarding preprocessing and feature selection algorithms e.g. by the using phases between EEG channel/frequency band combinations rather than spectral powers, using phase amplitude coupling strengths in channel/frequency band combinations with following Chow-Liu tree identification.
2) Furthermore, the graphical model itself can be modified/changed e.g. by approaches which allows cycles in information flows between nodes. Further investigation would be the approximation of dynamical graphical models e.g. conditional Chow-Liu trees and HMM's (Hidden Markov Models).
3) Combination of the two.

5. Conclusion

In this paper we introduce a novel method for the evaluation of neonatal brain function via multivariate EEG signal processing and embedding into a Chow-Liu tree. Identification of "distances" between EEG recordings of infants in a feature space which have been estimated from the multidimensional EEG signals was the main goal of this research. We show that by the algorithm constructed, features contain information regarding deviations from normal states of neonatal brains. Furthermore, we were able to make a visual proof on a 3d multidimensional scaling coordinate system with a good performance, reflecting that the distances (graph edit distance) between Chow-Liu trees of different infants are proportional to the clinical EEG findings of corresponding patients with pathological recordings. The patients with pathological EEG findings have Chow-Liu trees with small distance to each other in the 3d MDS Euclidean space.

More patient data is needed to improve the information extraction capabilities of the proposed method. Due to the inclusion of more EEG recordings we will improve the significance of the clusters already detected in the Euclidean space. On the other hand, we will be able to build new clusters of patients with similar (maybe unknown) characteristics in EEG linking maybe to similar clinical observations. By a structured and prospective assessment of infants of different gestational age, we expect to be able to show maturational effects and effects of influencing clinical factors on brain condition of preterm or newborn infants.

Declaration of Competing Interest

None.

Acknowledgements

This work was funded by the German Federal Ministry of Education and Research (reference number:13GW0033B, TENECOR).

Appendix

A.1. Data analysis

The idea behind this paper is the identification of a multivariate dependency structure of the 12 EEG channel recordings from newborns. Because of high complexity of such a data we decided to generate dependency trees, which were based on discretized data coming from frequency domain analysis. This decision is based on evidences (Niemarkt et al., 2008; Canolty et al., 2006) that the main information regarding the brain maturation state in neonatology can be extracted in frequency domains.

In first step we made short time Fourier transformation of the EEG channel data and generated corresponding spectrograms. An estimate of the power spectral density (PSD) (which builds spectrogram) is the so called periodogram. In our application to ensure the consistency of the PSD estimate we decided to use the well-known Welch's method.

In a second step we discretized the frequency range (with significant information content (Niemarkt et al., 2008)) between 0.25–31 Hz in 12 frequency bands (see Fig. A1). Since reliable estimation of powers in infraslow (<0.25 Hz) frequencies would require a perfectly DC stable and artifact-free EEG recording we decided to exclude them from the present work. For each frequency band we estimated the averaged integrated spectral power for each time window of the short time Fourier transform. In the last data generation step we discretized the accumulated spectral band powers in four groups by quantiles. Quantile method guarantees that each bin (four in our case) receives an equal number of data values and the data range of each bin varies according to the data values it contains. By this we got 12 channels times 12 frequency bands = 144 dimensional data set with discrete values {1,2,3,4}. The values of each 144 constructed frequency domain channels in a particular time window are corresponding to the strength of energy of a particular frequency band in a particular channel. We used 17.5 minutes sequences of the EEG data.

To accomplish the above described data generation steps, we had to set two main parameters of the short time Fourier transform, the window size of the Hamming window and the overlap time between Hamming windows. As the minimum frequency we want to resolve is 0.25 Hz, the corresponding minimum time window should be 4 s (the Rayleigh frequency).

For time windows that are relatively wide in their domain (such as Hamming window which is used here), 50% is a commonly used value for the overlap. With the data set generated in this manner

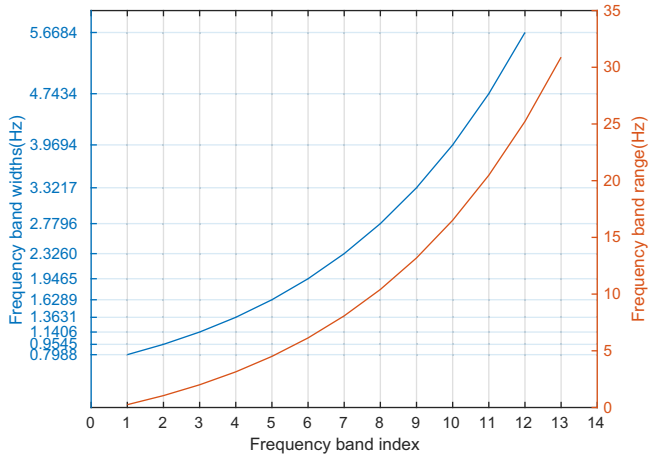

Fig. A1. Frequency range decomposition in 12 frequency bands (FB). We choose non uniform decomposition of FB. The orange y-axis shows the frequency range under consideration and the blue y-axis shows the corresponding widths of the FB. The x-axis shows the index of the 12 FB (e.g. Frequency band 5 begins at 5 Hz and has a width of 1.6289 Hz.).

we estimated one Chow-Liu tree for each patient recording, altogether 28 patients. Fig. 2a and Fig. 2b show two different Chow-Liu trees.

A.2. Chow-Liu trees based feature construction

Chow and Liu developed a method for approximation of joint probability distribution functions of a set of discrete variables using products of probability distributions involving no more than two different variables (Chow and Liu, 1968). Applying this method to the analysis of EEG recordings can be translated into the construction of a graphical representation of all EEG characteristics and the strengths of their respective interdependencies. The nodes in the estimated Chow-Liu trees are the channel/frequency band combinations and the edges indicate the generic dependencies between the signal energies in corresponding two nodes. The full tree is the factorization of the common probability distribution function of all 144 constructed discrete valued channels in frequency domain.

Some algorithms are generating tree-structured distributions and are able to reflect more complex dependencies (e.g., thin junction trees (Bach and Jordan 2003)). However, these algorithms have a higher time complexity than the Chow-Liu algorithm and do not guarantee optimality within the model class for the structure that is learned. Furthermore Chow-Liu trees have the following advantages: Good properties of probabilistic inference, as the tree is equal to its junction tree, furthermore the number of parameters are linear in dimensionality of the space (if one changes the structure of the trees by addition of only one more variable into the product terms of conditional distributions, the problem becomes non-deterministic polynomial-time (NP)-hard (Srebro, 2003)) and the simple intuitive interpretation of the resulting tree structure.

Assume $P(x)$ is the probability distribution function on discrete variables $\mathrm{x} = (\mathrm{x}_1, \mathrm{x}_2, \ldots, \mathrm{x}_\mathrm{n}), \mathrm{x}_\mathrm{i} \in \mathbb{N}^\mathrm{d}$ (in this paper x is the $d = 144$ dimensional vector of signal energies in channel/frequency band combinations measured n times)The chain rule is:

$$P(x) = p(x_1)\prod_{i=2}^{d} p(x_i|x_{i+1}, \ldots, x_d)$$

In the following we specify that the vector x with distribution $P(x)$ is Markovian on the graph $G = (V, E)$ if: $P(x_i|x_{nbd(i)}) = P(x_i|x_{V/i}), \forall i \in V$. Here $x_{nbd(i)}$ is the neighborhood of the variable x_i, i. e. $nbd(i) := \{j \in V : (i,j) \in E\}$ and $x_{V/i}$ are all remaining variables excluding the variable x_i. The graph $G = (V, E)$ is a tree if it is connected and acyclic. It is called forest with k edges and d nodes if it is acyclic and if $0 \leq k \leq d - 1$.

Assumption:. In the following we assume that the true distribution function P(x) is a forest structured distribution.

Chow and Liu constructed a distribution $T(x)$ for which the corresponding Markov network is a tree $G_T = (V, E_T)$ i. e. the joint distribution function can be written as a product of second order marginals $T(x) \propto \prod_{(u,v)\in E_T} T(x_u, x_v)$. A tree is a connected undirected graph that has no cycles. A spanning tree of a graph is a spanning graph which itself is a tree. Due to the fact that the interaction between the features (in terms of energy dependency between channel-frequency band combinations) does not have clear directionality we decided to use the Chow-Liu trees which are undirected graphical models.

If $G_T = (D, E_T)$ is the Markov network of probability distribution function T, then:

$$T(x) = \prod_{(u,v)\in E_T} \frac{T(x_u, x_v)}{T(x_v)T(x_u)} \prod_{v\in V} T(x_v)$$

Chow and Liu showed that the Kullback-Leibler divergence between $P(x)$ and $T(x)$ (see equation) is defined as: $KL(P, T) = \sum_x P(x)\log(P(x)/T(x))$ is minimal if the edges of the tree E_T maximizes the total mutual information of the tree. This is achieved by solving the maximum spanning tree problem with pairwise mutual information between variable edges as weights. Mutual information between two discrete random variables is calculated as follows: $I(x_u, x_v) = \sum_{x_u}\sum_{x_v} P(x_u, x_v)\log(P(x_u, x_v)/P(X_u)$ $P(x_v)$. The weighted undirected graph is $G((V, E)|w)$ in which w represents non-negative real numbers defined on the edges$(j, k) \in E$. The weight in the Chow-Liu trees are defined by the sum of mutual information between corresponding random variables (nodes) $W_T = \sum_{(u,v)\in E_T} I(x_u, x_v)$. To estimate the Chow-Liu tree from the data we used the Kruskaĺs minimum weight spanning tree algorithm (MWST) (Kruskal, 1958). However, there is a question about the statistical significance of the output of Kruskaĺs MWST algorithm, needless to say that the method will generate a tree also for random data. Therefore to find a trade-off between accuracy of the Chow-Liu tree structure and the description of the data i.e. to prune the Chow-Liu tree in an optimal manner we used the Chow-Liu threshold algorithm described by (Tan et al., 2011).

A.3. Model adaption and improvement

We used 17.5 min EEG signals (equivalent to the 506 data points) for Chow-Liu tree estimation. Several factors affect the correctness of the discovered Chow-Liu tree, including: quality of the available data, number of samples and strength of the causal relationships (mutual information) between Chow-Liu tree nodes. However, from (Canolty et al., 2006) we know how the number of nodes d (in our case 144 nodes, 12 frequency bands times 12 EEG channel signals) and the number of edges (in our case $< d - 1$ because of forest structure generated from a tree) can scale with n (the number of observed data), while maintaining the consistency (i. e. rate of probability at which the error event of structure learning decays to zero as $n \to \infty$). Under typical regularity conditions, e.g. described in (Wainwright et al., 2006), it can be shown that if $n = O(\log d)$, then the error probability of incorrectly learning the sequences of edges tends to zero as $n, d \to \infty$. In other words the number of nodes can grow faster than any polynomial in the sample size n (see also (Tan et al., 2011)).

References

André M, Lamblin MD, d'Allest AM, Curzi-Dascalova L, Moussalli-Salefranque F, Nguyen The Tich S, et al. Electroencephalography in premature and full-term infants. Developmental features and glossary. Neurophysiol Clin 2010;40:59–124.

Bach FR, Jordan MI. Beyond independent components: trees and clusters. J Mach Learn Res 2003;4:1205–33.

Canolty RT, Edwards E, Dalal SS, Soltani M, Nagarajan SS, Kirsch HE, et al. High gamma power is phase-locked to theta oscillations in human neocortex. Science 2006;313:1626–8.

Chow C, Liu C. Approximating discrete probability distributions with dependence trees. IEEE Trans Inform Theor 1968;14:462–7.

Curzi-Dascalova L, Figueroa JM, Eiselt M, Christova E, Virassamy A, d'Allest AM, et al. Sleep state organization in premature infants of less than 35 weeks' gestational age. Pediatr Res 1993;34:624–8.

Gao X, Bing X, Tao D, Xi Li. A survey of graph edit distance. Pattern Anal Appl 2010;13:113–29.

Gressens P, Rogido M, Paindaveine B, Sola A. The impact of neonatal intensive care practices on the developing brain. J Pediatr 2002;140:646–53.

Hayakawa F, Okumura A, Kato T, Kuno K, Watanabe K. Determination of timing of brain injury in preterm infants with periventricular leukomalacia with serial neonatal electroencephalography. Pediatrics 1999;104:1077–81.

Hellstrom-Westas L, Rosen I. Electroencephalography and brain damage in preterm infants. Early Hum Dev 2005;81:255–61.

Kruskal JB. On the shortest spanning subtree of a graph and the traveling selesman problem. Proc Am Math Soc 1958;7:48–50.

Lombroso CT. Neonatal polygraphy in full-term and premature infants: a review of normal and abnormal findings. J Clin Neurophysiol 1985;2:105–55.

Mormann F, Lehnertz K, David P, Elger ChE. Mean phase coherence as a measure for phase synchronization and its application to the eeg of epilepsy patients. Physica D 2000;144:358–69.

Niemarkt HJ, Andriessen P, Pasman J, Vles JS, Zimmermannn LJ, Oetomo SB. Analyzing EEG maturation in preterm infants: The value of a quantitative approach. J Neonatal Perinatal Med 2008;1:131–44.

Okumura A, Hayakawa F, Kato T, Kuno K, Watanabe K. Developmental outcome and types of chronic-stage EEG abnormalities in preterm infants. Dev Med Child Neurol 2002;44:729–34.

Perlman J. Neurobehavioral deficits in premature graduates of intensive care–potential medical and neonatal environmental risk factors. Pediatrics 2001;108:1339–48.

Pezzani C, Radvanyi-Bouvet MF, Relier JP, Monod N. Neonatal electroencephalography during the first twenty-four hours of life in full-term newborn infants. Neuropediatrics 1986;17:11–8.

Ryan T, Canolty CF, Koepsell K, Knight RT, Carmena JM. Multivariate phase-amplitude cross-frequency coupling in neurophysiological signals. IEEE Trans Biomed Eng 2012;59:8–11.

Scher MS, Martin JG, Steppe DA, Banks DL. Comparative estimates of neonatal gestational maturity by electrographic and fetal ultrasonographic criteria. Pediatr Neurol 1994;11:214–8.

Srebro N. Maximum Likelihood bounded tree-width markov networks. Artif Intell 2003;143:123–38.

Tan VYF, Anandkumar A, Willsky AS. Learning high-dimensional markov forest distributions: analysis of error rates. J Mach Learn Res 2011;12:1617–53.

Tort AB, Komorowski R, Eichenbaum H, Kopell N. Measuring phase-amplitude coupling between neuronal oscillations of different frequencies. J Neurophysiol 2010;104:1195–210.

Victor S, Appleton RE, Beirne M, Marson AG, Weindling AM. Spectral analysis of electroencephalography in premature newborn infants: normal ranges. Pediatr Res 2005;57:336–41.

Wainwright MJ, Ravikumar P, Lafferty JD. High-dimensional graphical model selection using -l_1-regularized logistic regression. Advances of Neural Information Processing Systems (NIPS) 2006;19. p. 1465–2147.

Watanabe K, Hayakawa F, Okumura A. Neonatal EEG: a powerful tool in the assessment of brain damage in preterm infants. Brain Dev 1999;21:361–72.

West CR, Harding JE, Williams CE, Gunning MI, Battin MR. Quantitative electroencephalographic patterns in normal preterm infants over the first week after birth. Early Hum Dev 2006;82:43–51.